IEEE Access
Multidisciplinary | Rapid Review | Open Access Journal

Received 7 June 2022, accepted 22 June 2022, date of publication 1 July 2022, date of current version 20 July 2022.

*Digital Object Identifier 10.1109/ACCESS.2022.3187712*

RESEARCH ARTICLE

# Fuzzy Adaptive Finite-Time Tracking for Hypersonic Flight Vehicles Using Switching Event-Triggered Methodology

**XINLEI TANG, DI SHEN, FUPING YU, AND MAOLONG LV**
Air Traffic Control and Navigation School, Air Force Engineering University, Xi'an 710051, China

Corresponding author: Di Shen (shendi1103@163.com)

This work was supported in part by the Young Talent Fund of Association for Science and Technology, Shaanxi, China, under Grant 20220101.

**ABSTRACT** The problem of event-triggered fuzzy adaptive finite-time tracking for flexible hypersonic flight vehicles is considered in this work. A new switching event-triggered mechanism is devised to mitigate the unnecessary resources waste in the process of system communication and sampled data computation. Compared with the traditional event-triggered mechanism, an exponential term with regard to tracking error is introduced into the proposed switching event-triggered function, which significantly reduces the frequencies of data transmission. To evade singularity issue typical of traditional recursive finite-time design methods, we introduce a new piecewise switching controller whose continuity and differentiability are ensured everywhere via an appropriate design. Stability of the proposed design is proved using asymmetric barrier Lyapunov functions, which are devised to tackle the fact that the operating regions of the flight state variables are asymmetric in actual engineering. Finally, comparative simulations are designed to illustrate the effectiveness and superiority of the presented methodology.

**INDEX TERMS** Switching event-triggered mechanism, singularity-free design, hypersonic flight vehicle, finite-time stability.

## I. INTRODUCTION

In recent decades, hypersonic flight vehicles (HFVs) equipped with air-breathing supersonic combustion ramjet (scramjets) have been widely researched owing to their excellent advantages in flight speed, penetration ability, and cost-effectiveness [1]–[4]. In order to reinforce the control performance, tremendous advanced control schemes have been resorted successively for HFVs dynamics, such as sliding-mode control [5], robust control [6], fault-tolerant control [7], and adaptive backstepping control [8]. However, it is worth noting that most of the existing results [5]–[8] can only realize infinite-time tracking, which implies that the system tracking error converge into an user-defined compact set when time goes to infinite. In view of high flight speed of HFVs exceeding Mach 5, fast convergence rate is necessary for hypersonic flight control.

To further enhance system convergence speed, the so-called finite-time tracking control methodology has been skillfully developed for the nonstrict-feedback systems [9], nontriangular stochastic systems [10], discrete time switched linear systems [11], and so on. To list a few, the finite-time adaptive fuzzy decentralized control problem is addressed in [9] for a class of interconnected large scale nonstrict-feedback systems with output constraint. In [10], the stochastically finite-time control issue is solved for a class of stochastic nontriangular systems. The problems of finite-time extended dissipative analysis and non-fragile tracking control are researched in [11] for uncertain discrete-time systems in switched linear form. However, there exists an overlooked singularity issue in existing results [9]–[11], derived from the fact that the corresponding virtual and actual control laws designed at each step are possibly non-differentiable, as the tracking error approaches zero. Based on this, a singularity-free design going beyond the available designs need to be sought to guarantee the finite-time stability, while guaranteeing the controller to be continuous and differentiable.

On the other hand, to mitigate the communication burden while guaranteeing satisfactory control performance, the

The associate editor coordinating the review of this manuscript and approving it for publication was Mou Chen.

event-triggered control technique [12]–[16] has been receiving more and more attention gradually compared with the classical periodic sampling control strategy. For example, Xu and Ma [13] investigated event-triggered exponential synchronization for a class of master-slave chaotic Lur'e systems. The relative position coordinated control problem is investigated in [14] for a class of uncertain spacecraft formation system flying under an undirected communication graph. In [15], a distributed adaptive control method is presented for a group of nonlinear systems under directed communication condition with event-triggered communication strategy. On account of the fixed and relative threshold strategy, Xing and Wen [16] propose a novel algorithm called the switching threshold strategy. However, the switching event-triggered mechanism proposed in [16] do not synthetically consider the effects of transient performances on inter-execution intervals. To this end, it is necessary to further develop a new error-dependent switching event-triggered mechanism to further mitigate the unnecessary resources waste in the process of system communication and sampled data computation. Motivated by above observations, the main contributions of this paper are listed in the following three-folds:

1) In contrast to the existing event-triggered mechanism [12]–[16], we develop a new switching event-triggered mechanism in the sense that introducing an exponential term with regard to tracking error into the switching event-triggered function, reducing the frequencies of data transmission significantly.
2) Different from traditional recursive finite-time design methods [9]–[11], we skillfully avoid the potential singularity issue by introducing a piecewise switching controller that guarantees the continuity and differentiability everywhere via an appropriate design.
3) In addition to solving singularity issue, some system states are constrained within some asymmetric sets by using asymmetric barrier Lyapunov functions. Remarkably, constrained flight state variables can also preserve the validity of fuzzy logic systems.

The rest of this paper is arranged in the following organization. Section II gives the preliminaries and problem statement. The finite-time fuzzy adaptive control design is devised in Section III. Section IV as well as Appendix show the stability analysis. Comparative simulations are provided in Section V to illustrate the effectiveness and superiority of the presented methodology. Section VI summarizes our paper finally.

## II. PRELIMINARIES AND PROBLEM STATEMENT

### A. HFVs LONGITUDINAL DYNAMICS MODEL

The considered HFVs longitudinal dynamic can be formulated as [17]–[19]:

$$\dot{V} = \frac{T\cos(\theta-\gamma)-D}{m} - g\sin\gamma, \tag{1}$$

$$\dot{h} = V\sin\gamma, \tag{2}$$

$$\dot{\gamma} = \frac{L+T\sin(\theta-\gamma)}{mV} - \frac{g}{V}\cos\gamma, \tag{3}$$

$$\dot{\theta} = Q, \tag{4}$$

$$\dot{Q} = \frac{M+\tilde{\psi}_1\ddot{\eta}_1+\tilde{\psi}_2\ddot{\eta}_2}{I_{yy}}, \tag{5}$$

$$k_1\ddot{\eta}_1 = -2\zeta_1\omega_1\dot{\eta}_1 - \omega_1^2\eta_1 + N_1 - \tilde{\psi}_1\frac{M}{I_{yy}} - \frac{\tilde{\psi}_1\tilde{\psi}_2\ddot{\eta}_2}{I_{yy}}, \tag{6}$$

$$k_2\ddot{\eta}_2 = -2\zeta_2\omega_2\dot{\eta}_2 - \omega_2^2\eta_2 + N_2 - \tilde{\psi}_2\frac{M}{I_{yy}} - \frac{\tilde{\psi}_2\tilde{\psi}_1\ddot{\eta}_1}{I_{yy}}, \tag{7}$$

where $T$, $D$, $L$, $M$, $N_1$ and $N_2$ are the thrust force, drag force, lift force, pitching moment, the first generalized force, and the second generalized force, respectively. The above forces and moment are defined as:

$$\begin{aligned}
T &= \beta_1(h,\bar{q})\Phi\alpha^3+\beta_2(h,\bar{q})\alpha^3+\beta_3(h,\bar{q})\Phi\alpha^2+\beta_4(h,\bar{q})\alpha^2\\
&\quad+\beta_5(h,\bar{q})\Phi\alpha+\beta_6(h,\bar{q})\alpha+\beta_7(h,\bar{q})\Phi+\beta_8(h,\bar{q}),\\
D &= \bar{q}S\left(C_D^{\alpha^2}\alpha^2+C_D^{\alpha}\alpha+C_D^0\right),\\
L &= \bar{q}S\left(C_L^{\alpha}\alpha+C_L^{\delta_e}\delta_e+C_L^0\right),\\
M &= z_T T+\bar{q}S\bar{c}\left(C_{M,\alpha}^{\alpha^2}\alpha^2+C_{M,\alpha}^{\alpha}\alpha+C_{M,\alpha}^0+c_e\delta_e\right),\\
N_1 &= N_1^{\alpha^2}\alpha^2+N_1^{\alpha}\alpha+N_1^0,\\
N_2 &= N_2^{\alpha^2}\alpha^2+N_2^{\alpha}\alpha+N_2^{\delta_e}\delta_e+N_2^0,\\
\bar{q} &= \frac{1}{2}\bar{\rho}V^2,\ \bar{\rho}=\bar{\rho}_0\exp\left(\frac{h_0-h}{h_s}\right).
\end{aligned}$$

Model (1)-(7) has been widely adopted in related literature (e.g. [17]–[19]): it contains 5 rigid body states (velocity $V$, altitude $h$, flight path angle $\gamma$, pitch angle $\theta$, and pitch rate $Q$), 2 flexible states ($i$-th generalized flexible coordinate $\eta_i$, $i=1,2$), and 2 control inputs (fuel equivalence ratio $\Phi$ and elevator angular deflection $\delta_e$). For more details on the various parameters, the reader is referred to [17].

### B. MODEL DECOMPOSITION

Along the similar model decomposition strategy as in [20], we can derive the velocity subsystem as follows

$$\dot{V} = f_V(V)+g_V(V)\Phi, \tag{8}$$

where $g_V=\cos\alpha\left[\beta_1(h,\bar{q})\alpha^3+\beta_3(h,\bar{q})\alpha^2+\beta_5(h,\bar{q})\alpha+\beta_7(h,\bar{q})\right]/m$, $f_V=-\bar{q}S\left(C_D^{\alpha^2}\alpha^2+C_D^{\alpha}\alpha+C_D^0\right)/m-g\sin\gamma+\cos\alpha\left[\beta_2(h,\bar{q})\alpha^3+\beta_4(h,\bar{q})\alpha^2+\beta_6(h,\bar{q})\alpha+\beta_8(h,\bar{q})\right]/m$. It is worth mentioning that, due to parametric uncertainty, the nonlinear functions $f_V$ and $g_V$ are unknown and cannot be used for control design.

Literature typically simplifies the altitude subsystem (2)-(7) by considering small flight path angles ($\sin\gamma\approx\gamma$) [17]–[20]. This results in

$$\begin{cases}\dot{h}=V\gamma, & \dot{\gamma}=f_\gamma(h,\gamma)+g_\gamma(h)\theta,\\ \dot{\theta}=Q, & \dot{Q}=f_Q(h,\gamma,\theta)+g_Q(h)\delta_e,\end{cases} \tag{9}$$

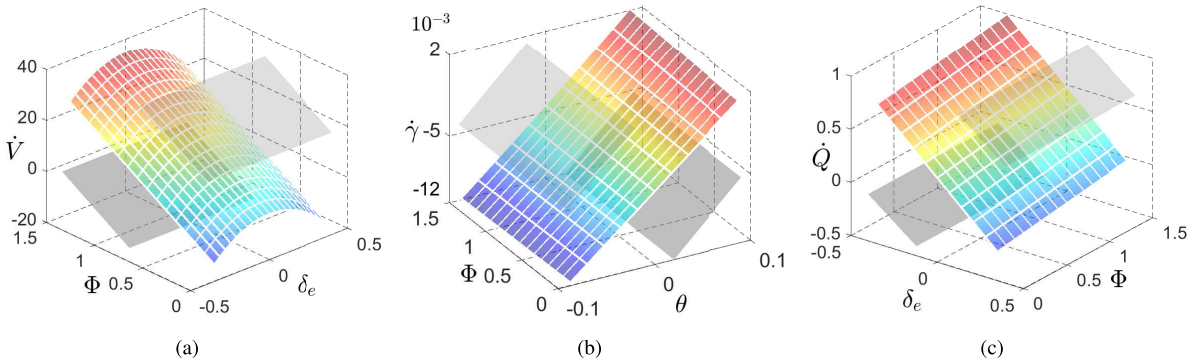


**FIGURE 1.** (a) The responses of $\dot{V}$ along with the varying of $\Phi$ and $\delta_e$; (b) The trajectories of $\dot{\gamma}$ along with the varying of $\Phi$ and $\theta$; (c) The evolutions of $\dot{Q}$ along with the varying of $\Phi$ and $\delta_e$.

where the functions $f_\gamma = \big(\bar{q}S(C_L^0 - C_L^\alpha\gamma) + T\sin\alpha\big)/(mV) - g\cos\gamma/V$, $g_\gamma = \bar{q}SC_L^\alpha/(mV)$, $f_Q = \big(z_T T + \bar{q}S\bar{c}C_{M,\alpha}(\alpha) + \tilde{\psi}_1\ddot{\eta}_1 + \tilde{\psi}_2\ddot{\eta}_2\big)/I_{yy}$, and $g_Q = \bar{q}S\bar{c}c_e/I_{yy}$ are also unknown due to parametric uncertainty and cannot be used for control design. Along the standard ideas as [17]–[20], we assume that there exist positive lower bounds $\underline{g}_V$, $\underline{g}_\gamma$, $\underline{g}_Q$, and positive upper bounds $\overline{g}_V$, $\overline{g}_\gamma$, $\overline{g}_Q$ such that $\underline{g}_V \le g_V \le \overline{g}_V$, $\underline{g}_\gamma \le g_\gamma \le \overline{g}_\gamma$ and $\underline{g}_Q \le g_Q \le \overline{g}_Q$.

*Remark 1:* Using the aerodynamic data from [17], Fig. 1 demonstrates that the decomposition method is meaningful. More specifically, Fig. 1(a) shows that $\dot{V}$ is affected by input $\Phi$ much more than input $\delta_e$, whereas Fig. 1(c) shows that $\dot{Q}$ is affected by input $\delta_e$ much more than input $\Phi$. Finally, Fig. 1(b) shows that $\dot{\gamma}$ is mostly affected by the variable $\theta$, which can be considered as an intermediate control input to be appropriately designed.

It is worth mentioning that the states in (1)-(7) should operate in the asymmetric constrained regions as follows [8]:

$$\Omega = \Big\{85000 \le h \le 135000[\text{ft}],\ 7500 \le V \le 11500[\text{ft/s}],\\ -5 \le \theta \le 10[\text{deg}],\ -10 \le Q \le 10[\text{deg/s}],\ -5 \le \gamma \le 7[\text{deg}]\Big\}.$$

We shall handle such asymmetric regions through asymmetric thresholds $-k_{a_\star}$ (lower threshold) and $k_{b_\star}$ (upper threshold) for the corresponding state tracking errors (in the following, the symbol $\star$ will be used as a short notation for the subscripts $V$, $h$, $\theta$, $\gamma$, and $Q$). The goal of this work is to develop the tracking controllers $\Phi$ and $\delta_e$ for system (1)-(7) such that the system outputs $V$ and $h$ follow the reference commands $V_{ref}$ and $h_{ref}$ within finite time, while the asymmetric state constraints are not violated.

At this stage, we shall introduce some technical lemmas, which are used for stability analysis.

*Lemma 1 [21]:* Consider the Lyapunov characterization of finite-time stability in the form $\dot{L}(x) \le -\varsigma_1 L(x) - \varsigma_2 L^l(x)$, where $\varsigma_1 > 0$, $\varsigma_2 > 0$, and $0 < l < 1$ are any real numbers. Then, $L(x)$ is convergent to a residual set with a finite settling time $T_0 \le \varsigma_1^{-1}(1-l)^{-1}\ln\Big[\big(\varsigma_1 L^{1-l}(x_0) + \varsigma_2\big)\varsigma_2^{-1}\Big]$.

*Lemma 2 [22]:* For $x, y \in \mathbb{R}$, if $0 < l = l_1/l_2 < 1$ with $l_1$ and $l_2$ being positive odd integers, then the inequality $xy^l \le -\xi x^{1+l} + \zeta(x+y)^{1+l}$ holds, where $\xi = (1+l)^{-1}\big(2^{l-1} - 2^{(l-1)(l+1)}\big)$, $\zeta = (1+l)^{-1}\big[(1+l)^{-1}l + 1 - 2^{(l-1)} + (1+l)^{-1}2^{-(l-1)^2(l+1)}\big]$.

## III. CONTROL DESIGN FOR HFVs DYNAMICS

### A. VELOCITY CONTROL DESIGN

Define the velocity tracking error $z_V = V - V_{ref}$, and design the following asymmetric BLF candidate:

$$L_V = \frac{1}{2}\hbar(z_V)\ln\frac{k_{bV}^2}{k_{bV}^2 - z_V^2} + \frac{1}{2}\big(1 - \hbar(z_V)\big)\ln\frac{k_{aV}^2}{k_{aV}^2 - z_V^2}, \tag{10}$$

where $\ln(\cdot)$ represents the natural logarithm of $\cdot$, and

$$\hbar(\cdot) \triangleq \begin{cases} 1, & \text{if } \cdot > 0, \\ 0, & \text{if } \cdot \le 0, \end{cases} \tag{11}$$

Hereafter, we abbreviate $\hbar(\cdot)$ by $\hbar$ for convenience. According to Lemma 2 of [24], $L_V$ in (10) is positive definite and differentiable in the set $z_V \in (-k_{aV}, k_{bV})$. According to (8) and (10) that the time derivative of $L_V$ is

$$\dot{L}_V = \Big(\frac{\hbar}{k_{bV}^2 - z_V^2} + \frac{1-\hbar}{k_{aV}^2 - z_V^2}\Big)z_V g_V \check{\Phi} + z_V F_V(\boldsymbol{x}_V), \tag{12}$$

where unknown dynamics $F_V(\boldsymbol{x}_V) = \big(\frac{\hbar}{k_{bV}^2 - z_V^2} + \frac{(1-\hbar)}{k_{aV}^2 - z_V^2}\big) \times (f_V + g_V e_V - \dot{V}_{ref})$ with $\boldsymbol{x}_V = V$, $\check{\Phi}$ and $e_V$ will be defined later. According to [23], $F_V(\boldsymbol{x}_V)$ can be approximated by an fuzzy logic system (FLS) such as $F_V(\boldsymbol{x}_V) = \boldsymbol{W}_V^{*\mathrm{T}}\boldsymbol{\varphi}_V(\boldsymbol{x}_V) + \varepsilon_V$, where $\boldsymbol{W}_V^*$ is the optimal parameter vector, $\boldsymbol{\varphi}_V(\boldsymbol{x}_V)$ is the fuzzy basis function vector, $\varepsilon_V$ is the minimum fuzzy approximation error and there exists $\varepsilon_V^* \in \mathbb{R}^+$ such that $|\varepsilon_V| \le \varepsilon_V^*$.

The intermediate control law $\check{\Phi}$ can be devised as

$$\check{\Phi} = -c_V z_V - \kappa_V \phi_V(z_V) - \frac{\psi_V \mu_V z_V^3}{4} - \frac{\psi_V z_V^3 \hat{\Xi}_V \Theta_V}{4l_V^4}, \tag{13}$$

where $\psi_V = \hbar\left(k_{bv}^2 - z_V^2\right) + (1-\hbar)\left(k_{av}^2 - z_V^2\right)$, $c_V, \mu_V, \kappa_V$ are positive design constants, $\hat{\Xi}_V$ is the estimate of $\Xi_V = ||\boldsymbol{W}_V^*||^4$, $\Theta_V = ||\boldsymbol{\varphi}_V(\boldsymbol{x}_V)||^4$, and $\phi_V(z_V)$ is designed as

$$\phi_V(z_V) = \boldsymbol{S}^T(z_V)\boldsymbol{\Psi}(z_V), \tag{14}$$

where $\boldsymbol{S}(\cdot)$ is the following vector of switching functions (whose rationale is clarified in Remark 2)

$$\boldsymbol{S}(\cdot) = \begin{cases} [1,0,0,0]^T, & \text{if } \cdot \geq \tau_V, \\ [0,1,0,0]^T, & \text{if } 0 < \cdot < \tau_V, \\ [0,0,1,0]^T, & \text{if } -\tau_V < \cdot \leq 0, \\ [0,0,0,1]^T, & \text{if } \cdot \leq -\tau_V, \end{cases}$$

and $\boldsymbol{\Psi}(z_V) = \left[z_V^l\left(k_{bv}^2 - z_V^2\right)^p, \upsilon_{Vb}z_V^3 + o_{Vb}z_V^5, \upsilon_{Va}z_V^3 + o_{Va}z_V^5, z_V^l\left(k_{av}^2 - z_V^2\right)^p\right]^T$ with $\upsilon_{Va} = \tau_V^{l-3}\left(k_{av}^2 - \tau_V^2\right)^p - o_{Va}\tau_V^2$, $o_{Va} = (l-3)\tau_V^{l-5}\left(k_{av}^2 - \tau_V^2\right)^p/2 - \left(k_{av}^2 - \tau_V^2\right)^{-q} p\tau_V^{l-3}$, $\upsilon_{Vb} = \tau_V^{l-3}\left(k_{bv}^2 - \tau_V^2\right)^p - o_{Vb}\tau_V^2$, $o_{Vb} = (l-3)\tau_V^{l-5}\left(k_{bv}^2 - \tau_V^2\right)^p/2 - \left(k_{bv}^2 - \tau_V^2\right)^{-q} p\tau_V^{l-3}$, $0 < l = l_1/l_2 < 1$, $l_1$, $l_2$ being positive odd integers, $p = (1-l)/2$, $q = (1+l)/2$, and $\tau_V$ being a small positive constant.

Let us now design the adaptation law $\dot{\hat{\Xi}}_V$ as

$$\dot{\hat{\Xi}}_V = -\sigma_{V1}\rho_V\hat{\Xi}_V - \sigma_{V2}\rho_V\hat{\Xi}_V^l + \frac{\rho_V z_V^4\Theta_V}{4l_V^4}, \tag{15}$$

where $\sigma_{V1}$ and $\sigma_{V2}$ are positive design constants. By setting $\hat{\Xi}_V(0) \geq 0$, and noting that $\dot{\hat{\Xi}}_V \geq 0$ when $\hat{\Xi}_V(t) = 0$, we can get that $\hat{\Xi}_V(t) \geq 0$ for $\forall t > 0$.

A novel switching event-triggered mechanism is devised as follows:

$$\Phi(t) = \check{\Phi}(t_k), \quad \forall t \in [t_k, t_{k+1}), \quad k \in \mathbb{N}^+, \tag{16}$$

$$t_{k+1} = \inf\left\{t \in \mathbb{R}^+ \,\middle|\, t > t_k \wedge e_V(t_k,t) - \boldsymbol{M}^\top\left(\check{\Phi}(t)\,|\,\xi_V\right)\boldsymbol{Y}\left(\check{\Phi}(t)\right) \geq 0\right\}, \tag{17}$$

where sampling error $e_V(t_k,t) = \check{\Phi}(t_k) - \check{\Phi}(t)$, the switching function

$$\boldsymbol{M}\left(\check{\Phi}(t)\,|\,\xi_V\right) = \begin{cases} [1,\,0]^\top, & \text{if } |\check{\Phi}(t)| < \xi_V, \\ [0,\,1]^\top, & \text{otherwise}, \end{cases} \tag{18}$$

and vector function $\boldsymbol{Y}\left(\check{\Phi}(t)\right) = \left[\kappa_{V,1} + \rho_V|\check{\Phi}(t)| + \zeta_V(t), \kappa_{V,2}\right]^\top$ with $\kappa_{V,2} = c_{V,1}\exp(c_{V,0}) + \rho_V\xi_V + \kappa_{V,1}$, $\zeta_V(t) = c_{V,1}\exp(-z_V^2(t) + c_{V,0})$, $\rho_V < 1$, $\xi_V$, $\kappa_{V,1}$, $c_{V,0}$, and $c_{V,1}$ being positive design parameters. The details of the proposed threshold strategy can be found in Algorithm 1.

Substituting (13) and (16) into (12), and using the lower bound $\underline{g}_V$ yields

$$\dot{L}_V \leq -\frac{\hbar\kappa_V\underline{g}_V z_V\phi_V(z_V)}{k_{bv}^2 - z_V^2} - \frac{(1-\hbar)\kappa_V\underline{g}_V z_V\phi_V(z_V)}{k_{av}^2 - z_V^2} - \frac{\hbar c_V\underline{g}_V z_V^2}{k_{bv}^2 - z_V^2} - \frac{(1-\hbar)c_V\underline{g}_V z_V^2}{k_{av}^2 - z_V^2} + \frac{3l_V^{\frac{4}{3}}}{4}$$

**Algorithm 1:** Compute the Event-Triggered Signal

**Input :** Sliding mode tracking error $\check{\Phi}(t)$ and relative tracking error $z_V(t)$

**Output:** Event-triggered signal $\check{\Phi}(t_k)$

Initialize: $\check{\Phi}(t_0) = \check{\Phi}(0)$, $t_0 = 0$, $k = 1$, $M \in \mathbb{N}^+$

Choose positive design parameters $\xi_V$, $\kappa_{V,1}$, $\kappa_{V,2}$, $c_{V,0}$, $c_{V,1}$, and $\rho_V$, and positive continuous function

$$\zeta_V(t) = c_{V,1}\exp(-z_V^2(t) + c_{V,0})$$

```
for k = 1 → M do
    if |Φ̌(t)| < ξ_V then
        if |e_V(t_k, t)| ≥ κ_{V,1} + ρ_V|Φ̌(t)| + ζ_V(t) then
            Φ̌(t_k) = Φ̌(t), t_k = t, k = k + 1
        else if |e_V(t_k, t)| < κ_{V,1} + ρ_V|Φ̌(t)| + ζ_V(t) then
            Φ̌(t_k) = Φ̌(t_{k−1})
        end
    else if |Φ̌(t)| ≥ ξ_V then
        if |e_V(t_k, t)| ≥ κ_{V,2} then
            Φ̌(t_k) = Φ̌(t), t_k = t, k = k + 1
        else if |e_V(t_k, t)| < κ_{V,2} then
            Φ̌(t_k) = Φ̌(t_{k−1})
        end
    end
end
```

$$+\frac{z_V^4\tilde{\Xi}_V\Theta_V}{4l_V^4} + \frac{3\varepsilon_V^{*\frac{4}{3}}}{4(\mu_V\underline{g}_V)^{\frac{1}{3}}} - \frac{\mu_V\underline{g}_V z_V^4}{4} + \frac{z_V^4\tilde{\Xi}_V\Theta_V}{4l_V^4} + z_V\varepsilon_V, \tag{19}$$

where $\hat{\Xi}_V \geq 0$ and $\tilde{\Xi}_V = \Xi_V - \underline{g}_V\hat{\Xi}_V$, and $l_V$ is a positive design constant.

Applying Young's inequality to (19) yields

$$\dot{L}_V \leq -\frac{(1-\hbar)\kappa_V\underline{g}_V z_V\phi_V(z_V)}{k_{av}^2 - z_V^2} - \frac{\hbar\kappa_V\underline{g}_V z_V\phi_V(z_V)}{k_{bv}^2 - z_V^2} - \frac{\hbar c_V\underline{g}_V z_V^2}{k_{bv}^2 - z_V^2} - \frac{(1-\hbar)c_V\underline{g}_V z_V^2}{k_{av}^2 - z_V^2} + \frac{3l_V^{\frac{4}{3}}}{4} + \frac{z_V^4\tilde{\Xi}_V\Theta_V}{4l_V^4} + \frac{3\varepsilon_V^{*\frac{4}{3}}}{4(\mu_V\underline{g}_V)^{\frac{1}{3}}}. \tag{20}$$

which shall be utilized for stability analysis later.

*Remark 2:* Different from the traditional switching event-triggered mechanism [16], the key features of the presented design lie in introducing an error-dependent monotonically decreasing exponential term $\zeta_V(t)$ into the triggering function as in (17). This design can give a larger triggering threshold when tracking errors $z_V$ become small. In practical engineering, the too small inter-execution interval is unnecessary as long as good tracking performance has been realized.

### B. ALTITUDE CONTROL DESIGN

Because the altitude subsystem consists of four states, the control design requires four iterative steps. The first three

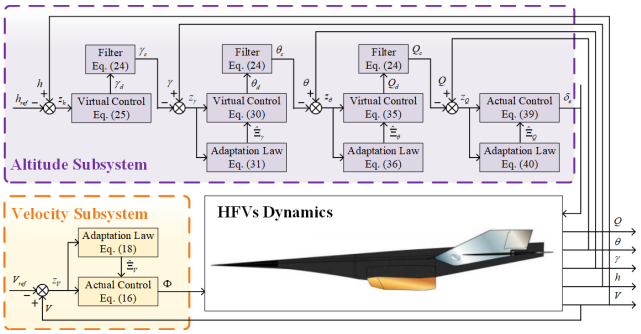


**FIGURE 2.** The framework of the proposed control structure.

steps are meant to design three virtual control laws $\gamma_d$, $\theta_d$, $Q_d$, whereas the last step is meant to design the actual control law $\delta_e$.

*Step 1:* Let us define the altitude tracking error $z_h = h - h_{ref}$, and design the following asymmetric BLF candidate:

$$L_h = \frac{1}{2}\hbar \ln \frac{k_{b_h}^2}{k_{b_h}^2 - z_h^2} + \frac{1}{2}(1-\hbar) \ln \frac{k_{a_h}^2}{k_{a_h}^2 - z_h^2}, \tag{21}$$

Recalling (9) and (21) gives

$$\dot{L}_h = \left( \frac{\hbar}{k_{b_h}^2 - z_h^2} + \frac{1-\hbar}{k_{a_h}^2 - z_h^2} \right) \left( z_h V\gamma - z_h \dot{h}_{ref} \right), \tag{22}$$

Define the following error dynamics:

$$\begin{cases} z_\gamma = \gamma - \gamma_c, \quad z_\theta = \theta - \theta_c, \quad z_Q = Q - Q_c, \\ y_\gamma = \gamma_c - \gamma_d, y_\theta = \theta_c - \theta_d, \ y_Q = Q_c - Q_d, \end{cases} \tag{23}$$

in which tracking errors $z_\gamma$, $z_\theta$, and $z_Q$, virtual control laws $\gamma_d$, $\theta_d$, and $Q_d$, boundary layer errors $y_\gamma$, $y_\theta$, and $y_Q$, and first-order filters outputs$\gamma_c$, $\theta_c$, and $Q_c$ are defined as follows

$$\begin{cases} \dot{\gamma}_c = -\tau_{\gamma 1} y_\gamma - \tau_{\gamma 2} y_\gamma^l, \\ \dot{\theta}_c = -\tau_{\theta 1} y_\theta - \tau_{\theta 2} y_\theta^l, \\ \dot{Q}_c = -\tau_{Q1} y_Q - \tau_{Q2} y_Q^l, \end{cases} \tag{24}$$

where $\tau_{\gamma 1}$, $\tau_{\gamma 2}$, $\tau_{\theta 1}$, $\tau_{\theta 2}$, $\tau_{Q1}$, $\tau_{Q2}$ are positive design parameters, and $0 < l = l_1/l_2 < 1$ with $l_1$, $l_2$ being positive odd integers.

Subsequently, let us devise the virtual control law $\gamma_d$ as

$$\gamma_d = -V^{-1} c_h z_h - V^{-1} \kappa_h \phi_h(z_h) - V^{-1} \dot{h}_{ref}, \tag{25}$$

where $c_h$, $\mu_h$, $\kappa_h$ are positive design constants, and $\phi_h(z_h)$ is designed as

$$\phi_h(z_h) = \boldsymbol{S}^T(z_h) \boldsymbol{\Psi}(z_h), \tag{26}$$

where $\boldsymbol{\Psi}(z_h) = \left[ z_h^l \left(k_{b_h}^2 - z_h^2\right)^p, \upsilon_{hb} z_h^3 + o_{hb} z_h^5, \upsilon_{ha} z_h^3 + o_{ha} z_h^5, z_h^l \left(k_{a_h}^2 - z_h^2\right)^p \right]^T$ with $\upsilon_{ha} = \tau_h^{l-3} (k_{a_h}^2 - \tau_h^2)^p - o_{ha} \tau_h^2$, $o_{ha} = (l-3)\tau_h^{l-5} \left(k_{a_h}^2 - \tau_h^2\right)^p / 2 - \left(k_{a_h}^2 - \tau_h^2\right)^{-q} p \tau_h^{l-3}$, $\upsilon_{hb} = \tau_h^{l-3} (k_{b_h}^2 - \tau_h^2)^p - o_{hb} \tau_h^2$, $o_{hb} = (l-3)\tau_h^{l-5} \left(k_{b_h}^2 - \tau_h^2\right)^p / 2 - \left(k_{b_h}^2 - \tau_h^2\right)^{-q} p \tau_h^{l-3}$, and $\tau_h$ being a small positive constant.

*Remark 3:* The introduction of switching function $\boldsymbol{S}(z_h)$ stems from the requirement for differentiability in finite-time control. Noticing that traditional methodologies typically devise $\phi_h(z_h) = z_h^l$ with $0 < l < 1$ for $\forall z_h \in \mathbb{R}$ to realize finite-time tracking [9]–[11]. However, this choice might lead to $\dot{\phi}_h(z_h) = l z_h^{l-1} \to \infty$ as $z_h \to 0$, causing a singularity issue. To overcome this singularity issue, we skillfully design the switching function $\phi_h(z_h)$ (26). For this function, we could reveal the continuity of $\phi_h$ and $\dot{\phi}_h$ such as:

$$\begin{aligned}
&\lim_{z_h \to \tau_h^-} \phi_h(z_h) = \lim_{z_h \to \tau_h^+} \phi_h(z_h) = \tau_h^l \left(k_{b_h}^2 - \tau_h^2\right)^p, \\
&\lim_{z_h \to \tau_h^-} \dot{\phi}_h(z_h) = \lim_{z_h \to \tau_h^+} \dot{\phi}_h(z_h) = \Big[ l \tau_h^{l-1} \left(k_{b_h}^2 - \tau_h^2\right)^p \\
&\qquad -2p\tau_h^{l+1} \left(k_{b_h}^2 - \tau_h^2\right)^{p-1} \Big] (V\gamma - \dot{h}_{ref}), \\
&\lim_{z_h \to 0^-} \phi_h(z_h) = \lim_{z_h \to 0^+} \phi_h(z_h) = 0, \\
&\lim_{z_h \to 0^-} \dot{\phi}_h(z_h) = \lim_{z_h \to 0^+} \dot{\phi}_h(z_h) = 0, \\
&\lim_{z_h \to -\tau_h^-} \phi_h(z_h) = \lim_{z_h \to -\tau_h^+} \phi_h(z_h) = -\tau_h^l \left(k_{a_h}^2 - \tau_h^2\right)^p, \\
&\lim_{z_h \to -\tau_h^-} \dot{\phi}_h(z_h) = \lim_{z_h \to -\tau_h^+} \dot{\phi}_h(z_h) = \Big[ l \tau_h^{l-1} \left(k_{a_h}^2 - \tau_h^2\right)^p \\
&\qquad -2p\tau_h^{l+1} \left(k_{a_h}^2 - \tau_h^2\right)^{p-1} \Big] (V\gamma - \dot{h}_{ref}).
\end{aligned}$$

which further guarantees the absence of the singularity issue in $\gamma_d$.

Similarly to Sect. III. A, substituting (25) into (22) and using $\gamma = e_\gamma + y_\gamma + \gamma_d$ yields

$$\begin{aligned}
\dot{L}_h = &\left( \frac{\hbar}{k_{b_h}^2 - z_h^2} + \frac{1-\hbar}{k_{a_h}^2 - z_h^2} \right) z_h V (z_\gamma + y_\gamma) \\
&- \frac{(1-\hbar)\kappa_h z_h \phi_h(z_h)}{k_{a_h}^2 - z_h^2} - \frac{\hbar \kappa_h z_h \phi_h(z_h)}{k_{b_h}^2 - z_h^2} \\
&- \frac{\hbar c_h z_h^2}{k_{b_h}^2 - z_h^2} - \frac{(1-\hbar) c_h z_h^2}{k_{a_h}^2 - z_h^2}.
\end{aligned} \tag{27}$$

According to (25) we can known that $\gamma_d$ and $\dot{\gamma}_d$ are two functions with respect to $z_h$, $\dot{h}_{ref}$ and $z_h$, $z_\gamma$, $y_\gamma$, $\dot{h}_{ref}$, $\ddot{h}_{ref}$, respectively. Owing to the presence of the smooth switching signal $\phi_h(z_h)$, functions $\gamma_d$ and $\dot{\gamma}_d$ are both continuous. Thus, we can get from (23) and (24) that $\dot{y}_\gamma = -\tau_{\gamma 1} y_\gamma - \tau_{\gamma 2} y_\gamma^l + \iota_\gamma(z_h, z_\gamma, y_\gamma, \dot{h}_{ref}, \ddot{h}_{ref})$ with $\iota_\gamma(\cdot)$ a continuous function.

*Step 2:* Let us design the BLF candidate as follows

$$L_\gamma = \frac{1}{2}\hbar \ln \frac{k_{b_\gamma}^2}{k_{b_\gamma}^2 - z_\gamma^2} + \frac{1}{2}(1-\hbar) \ln \frac{k_{a_\gamma}^2}{k_{a_\gamma}^2 - z_\gamma^2}. \tag{28}$$

Recalling (9) and (28) gives

$$\begin{aligned}
\dot{L}_\gamma \le &-\left( \frac{\hbar}{k_{b_h}^2 - z_h^2} + \frac{1-\hbar}{k_{a_h}^2 - z_h^2} \right) z_h V (z_\gamma + y_\gamma) + F_\gamma(\boldsymbol{x}_\gamma) \\
&+ \left( \frac{\hbar}{k_{b_\gamma}^2 - z_\gamma^2} + \frac{1-\hbar}{k_{a_\gamma}^2 - z_\gamma^2} \right) z_\gamma g_\gamma (z_\theta + y_\theta + \theta_d),
\end{aligned} \tag{29}$$

where unknown dynamics $F_\gamma(\boldsymbol{x}_\gamma) = \left(\frac{\hbar}{k_{b_\gamma}^2 - z_\gamma^2} + \frac{1-\hbar}{k_{a_\gamma}^2 - z_\gamma^2}\right) \times (f_\gamma - \dot{\gamma}_c) + (Vz_h y_\gamma / z_\gamma + Vz_h)\left(\frac{\hbar}{k_{b_h}^2 - z_h^2} + \frac{1-\hbar}{k_{a_h}^2 - z_h^2}\right)$ with $\boldsymbol{x}_\gamma = [h, \gamma] \in \mathbb{R}^2$. According to [23], $F_\gamma(\boldsymbol{x}_\gamma)$ can be approximated by an FLS as $F_\gamma(\boldsymbol{x}_\gamma) = \boldsymbol{W}_\gamma^{*\mathrm{T}} \boldsymbol{\varphi}_\gamma(\boldsymbol{x}_\gamma) + \varepsilon_\gamma$, where $\varepsilon_\gamma$ is the fuzzy approximation error and there exists $\varepsilon_\gamma^* \in \mathbb{R}^+$ such that $|\varepsilon_\gamma| \le \varepsilon_\gamma^*$.

Devise the virtual control law as well as the adaptation law as

$$\theta_d = -\frac{\psi_\gamma z_\gamma^3 \hat{\Xi}_\gamma \Theta_\gamma}{4 l_\gamma^4} - \frac{\psi_\gamma \mu_\gamma z_\gamma^3}{4} - \kappa_\gamma \phi_\gamma(z_\gamma) - c_\gamma z_\gamma, \quad (30)$$

$$\dot{\hat{\Xi}}_\gamma = -\rho_\gamma \sigma_{\gamma 1} \hat{\Xi}_\gamma - \rho_\gamma \sigma_{\gamma 2} \hat{\Xi}_\gamma^l + \frac{\rho_\gamma z_\gamma^4 \Theta_\gamma}{4 l_\gamma^4}, \quad (31)$$

where $\psi_\gamma = \hbar\left(k_{b_\gamma}^2 - z_\gamma^2\right) + (1-\hbar)\left(k_{a_\gamma}^2 - z_\gamma^2\right)$, $c_\gamma, \mu_\gamma, \kappa_\gamma, \rho_\gamma$, $\sigma_{\gamma 1}$, and $\sigma_{\gamma 2}$ are positive design constants, $\hat{\Xi}_\gamma$ is the estimate of $\Xi_\gamma = ||\boldsymbol{W}_\gamma^*||^4$ with $\hat{\Xi}_\gamma(0) \ge 0$, $\Theta_\gamma = ||\boldsymbol{\varphi}_\gamma(\boldsymbol{x}_\gamma)||^4$, and $\phi_\gamma(z_\gamma)$ is designed similar to (14) and (26).

Subsequently, along the similar steps as (27), one has

$$\begin{aligned}\dot{L}_\gamma \le & -\left(\frac{\hbar}{k_{b_h}^2 - z_h^2} + \frac{1-\hbar}{k_{a_h}^2 - z_h^2}\right) z_h V(z_\gamma + y_\gamma) + \frac{3\varepsilon_\gamma^{*\frac{4}{3}}}{4(\mu_\gamma \underline{g}_\gamma)^{\frac{1}{3}}} \\ & - \frac{\hbar c_\gamma \underline{g}_\gamma z_\gamma^2}{k_{b_\gamma}^2 - z_\gamma^2} - \frac{(1-\hbar) c_\gamma \underline{g}_\gamma z_\gamma^2}{k_{a_\gamma}^2 - z_\gamma^2} + \frac{z_\gamma^4 \tilde{\Xi}_\gamma \Theta_\gamma}{4 l_\gamma^4} + \frac{3 l_\gamma^{\frac{4}{3}}}{4} \\ & - \frac{\hbar \kappa_\gamma \underline{g}_\gamma z_\gamma \phi_\gamma(z_\gamma)}{k_{b_\gamma}^2 - z_\gamma^2} - \frac{(1-\hbar)\kappa_\gamma \underline{g}_\gamma z_\gamma \phi_\gamma(z_\gamma)}{k_{a_\gamma}^2 - z_\gamma^2} \\ & + \left(\frac{\hbar}{k_{b_\gamma}^2 - z_\gamma^2} + \frac{1-\hbar}{k_{a_\gamma}^2 - z_\gamma^2}\right) z_\gamma g_\gamma (z_\theta + y_\theta), \end{aligned} \quad (32)$$

with $\tilde{\Xi}_\gamma = \Xi_\gamma - \underline{g}_\gamma \hat{\Xi}_\gamma$ and $l_\gamma$ being a positive design constant. Similarly, in accordance with (23) and (24), we arrive $\dot{y}_\theta = -\tau_{\theta 1} y_\theta - \tau_{\theta 2} y_\theta^l + \iota_\theta(z_h, z_\gamma, z_\theta, \hat{\Xi}_\gamma, y_\gamma, y_\theta, h_{ref}, \dot{h}_{ref}, \ddot{h}_{ref})$ with $\iota_\theta(\cdot)$ being a continuous function.

*Step 3:* Design the BLF candidate as follows

$$L_\theta = \frac{1}{2}\hbar \ln \frac{k_{b_\theta}^2}{k_{b_\theta}^2 - z_\theta^2} + \frac{1}{2}(1-\hbar) \ln \frac{k_{a_\theta}^2}{k_{a_\theta}^2 - z_\theta^2}, \quad (33)$$

whose time derivative along (9) and (33) is

$$\begin{aligned}\dot{L}_\theta = & \left(\frac{\hbar}{k_{b_\theta}^2 - z_\theta^2} + \frac{1-\hbar}{k_{a_\theta}^2 - z_\theta^2}\right) z_\theta (z_Q + y_Q + Q_d) \\ & - \left(\frac{\hbar}{k_{b_\gamma}^2 - z_\gamma^2} + \frac{1-\hbar}{k_{a_\gamma}^2 - z_\gamma^2}\right) z_\gamma g_\gamma (z_\theta + y_\theta) \\ & + \frac{z_\theta^4 \Xi_\theta \Theta_\theta}{4 l_\theta^4} + \frac{3 l_\theta^{\frac{4}{3}}}{4} + z_\theta \varepsilon_\theta, \end{aligned} \quad (34)$$

where unknown dynamics $F_\theta(\boldsymbol{x}_\theta) = \left(\frac{\hbar}{k_{b_\gamma}^2 - z_\gamma^2} + \frac{1-\hbar}{k_{a_\gamma}^2 - z_\gamma^2}\right) \times (z_\gamma g_\gamma + z_\gamma g_\gamma y_\theta / z_\theta) - \left(\frac{\hbar}{k_{b_\theta}^2 - z_\theta^2} + \frac{1-\hbar}{k_{a_\theta}^2 - z_\theta^2}\right)\dot{\theta}_c$ with $\boldsymbol{x}_\theta = [h, \gamma, \theta] \in \mathbb{R}^3$. According to [23], $F_\theta(\boldsymbol{x}_\theta)$ can be approximated by an FLS as $F_\theta(\boldsymbol{x}_\theta) = \boldsymbol{W}_\theta^{*\mathrm{T}} \boldsymbol{\varphi}_\theta(\boldsymbol{x}_\theta) + \varepsilon_\theta$, where $\varepsilon_\theta$ is the fuzzy approximation error and there exists $\varepsilon_\theta^* \in \mathbb{R}^+$ such that $|\varepsilon_\theta| \le \varepsilon_\theta^*$.

Along Steps 1-2, devise the virtual control law as well as the adaptation law as

$$Q_d = -\frac{\psi_\theta z_\theta^3 \hat{\Xi}_\theta \Theta_\theta}{4 l_\theta^4} - \frac{\psi_\theta \mu_\theta z_\theta^3}{4} - \kappa_\theta \phi_\theta(z_\theta) - c_\theta z_\theta, \quad (35)$$

$$\dot{\hat{\Xi}}_\theta = -\rho_\theta \sigma_{\theta 1} \hat{\Xi}_\theta - \rho_\theta \sigma_{\theta 2} \hat{\Xi}_\theta^l + \frac{\rho_\theta z_\theta^4 \Theta_\theta}{4 l_\theta^4}, \quad (36)$$

where $\psi_\theta = \hbar\left(k_{b_\theta}^2 - z_\theta^2\right) + (1-\hbar)\left(k_{a_\theta}^2 - z_\theta^2\right)$, $c_\theta, \mu_\theta, \kappa_\theta, \rho_\theta$, $\sigma_{\theta 1}$, and $\sigma_{\theta 2}$ are positive design constants, $\hat{\Xi}_\theta$ is the estimate of $\Xi_\theta = ||\boldsymbol{W}_\theta^*||^4$ with $\hat{\Xi}_\theta(0) \ge 0$, $\Theta_\theta = ||\boldsymbol{\varphi}_\theta(\boldsymbol{x}_\theta)||^4$, and $\phi_\theta(z_\theta)$ is devised similar to (14) and (26).

Then, similar to (27), we arrive at

$$\begin{aligned}\dot{L}_\theta \le & -\frac{\hbar c_\theta z_\theta^2}{k_{b_\theta}^2 - z_\theta^2} - \frac{(1-\hbar) c_\theta z_\theta^2}{k_{a_\theta}^2 - z_\theta^2} - \frac{(1-\hbar)\kappa_\theta z_\theta \phi_\theta(z_\theta)}{k_{a_\theta}^2 - z_\theta^2} \\ & - \frac{\hbar \kappa_\theta z_\theta \phi_\theta(z_\theta)}{k_{b_\theta}^2 - z_\theta^2} + \frac{z_\theta^4 \tilde{\Xi}_\theta \Theta_\theta}{4 l_\theta^4} + \frac{3\varepsilon_\theta^{*\frac{4}{3}}}{4(\mu_\theta \underline{g}_\theta)^{\frac{1}{3}}} + \frac{3 l_\theta^{\frac{4}{3}}}{4} \\ & - \left(\frac{\hbar}{k_{b_\gamma}^2 - z_\gamma^2} + \frac{1-\hbar}{k_{a_\gamma}^2 - z_\gamma^2}\right) z_\gamma g_\gamma (z_\theta + y_\theta) \\ & + \left(\frac{\hbar}{k_{b_\theta}^2 - z_\theta^2} + \frac{1-\hbar}{k_{a_\theta}^2 - z_\theta^2}\right) z_\theta (z_Q + y_Q), \end{aligned} \quad (37)$$

where $\tilde{\Xi}_\theta = \Xi_\theta - \hat{\Xi}_\theta$, $l_\theta$ is a positive design constant, and $\dot{y}_Q = -\tau_{Q1} y_Q - \tau_{Q2} y_Q^l + \iota_Q(z_h, z_\gamma, z_\theta, z_Q, \hat{\Xi}_\gamma, y_\gamma, y_\theta, y_Q, h_{ref}, \dot{h}_{ref}, \ddot{h}_{ref})$ with $\iota_Q(\cdot)$ being a continuous function.

*Step 4:* Let us design the actual control law $\delta_e$ in this step. Construct the BLF candidate as follows

$$L_Q = \frac{1}{2}\hbar \ln \frac{k_{b_Q}^2}{k_{b_Q}^2 - z_Q^2} + \frac{1}{2}(1-\hbar) \ln \frac{k_{a_Q}^2}{k_{a_Q}^2 - z_Q^2}. \quad (38)$$

Similarly, let us design the intermediate actual control law as well as the adaptation law as

$$\begin{aligned}\check{\delta}_e = & -c_Q z_Q - \kappa_Q \phi_Q(z_Q) \\ & - \frac{\psi_Q z_Q^3 \hat{\Xi}_Q \Theta_Q}{4 l_Q^4} - \frac{\psi_Q \mu_Q z_Q^3}{4}, \end{aligned} \quad (39)$$

$$\dot{\hat{\Xi}}_Q = -\rho_Q \sigma_{Q1} \hat{\Xi}_Q - \rho_Q \sigma_{Q2} \hat{\Xi}_Q^l + \frac{\rho_Q z_Q^4 \Theta_Q}{4 l_Q^4}, \quad (40)$$

where $\psi_Q = \hbar\left(k_{b_Q}^2 - z_Q^2\right) + (1-\hbar)\left(k_{a_Q}^2 - z_Q^2\right)$, $c_Q, \mu_Q, \kappa_Q, \rho_Q$, $\sigma_{Q1}$, and $\sigma_{Q2}$ are positive design constants, $\hat{\Xi}_Q$ is the estimate of $\Xi_Q$ with $\hat{\Xi}_Q(0) \ge 0$, and $\phi_Q(z_Q)$ is designed similar to (14) and (26).

Similar to velocity subsystem, a novel switching event-triggered mechanism is devised as follows:

$$\delta_e(t) = \check{\delta}_e(t_k), \quad \forall t \in [t_k, t_{k+1}), \quad k \in \mathbb{N}^+, \quad (41)$$

$$t_{k+1} = \inf\Big\{t \in \mathbb{R}^+ \Big| t > t_k \wedge e_h(t_k, t) \\ -\boldsymbol{M}^\top\big(\check{\delta}_e(t)\,|\,\xi_h\big)\boldsymbol{Y}\big(\check{\delta}_e(t)\big) \geq 0\Big\}, \quad (42)$$

where sampling error $e_h(t_k, t) = \check{\delta}_e(t_k) - \check{\delta}_e(t)$, the switching function

$$\boldsymbol{M}\big(\check{\delta}_e(t)\,|\,\xi_h\big) = \begin{cases} [1,\ 0]^\top, & \text{if } |\check{\delta}_e(t)| < \xi_h, \\ [0,\ 1]^\top, & \text{otherwise}, \end{cases} \quad (43)$$

and $\boldsymbol{Y}\big(\check{\delta}_e(t)\big) = \big[\kappa_{h,1} + \rho_h|\check{\delta}_e(t)| + \zeta_h(t),\ \kappa_{h,2}\big]^\top$ with $\kappa_2 = c_{h,1}\exp(c_{h,0}) + \rho_h\xi_h + \kappa_{h,1}$, $\zeta_h(t) = c_{h,1}\exp(-z_h^2(t) + c_{h,0})$, $\rho_h < 1$, $\xi_h$, $\kappa_{h,1}$, $c_{h,0}$, and $c_{h,1}$ being positive design parameters.

Subsequently, along the similar steps as (27), one has

$$\dot{L}_Q \leq -\frac{\hbar c_Q \underline{g}_Q z_Q^2}{k_{b_Q}^2 - z_Q^2} - \frac{(1-\hbar)c_Q\underline{g}_Q z_Q^2}{k_{a_Q}^2 - z_Q^2} - \frac{\hbar\kappa_Q\underline{g}_Q z_Q\phi_Q(z_Q)}{k_{b_Q}^2 - z_Q^2} \\ -\frac{(1-\hbar)\kappa_Q\underline{g}_Q z_Q\phi_Q(z_Q)}{k_{a_Q}^2 - z_Q^2} + \frac{z_Q^4\tilde{\Xi}_Q\Theta_Q}{4l_Q^4} + \frac{3\varepsilon_Q^{*\frac{4}{3}}}{4(\mu_Q\underline{g}_Q)^{\frac{1}{3}}} \\ -\Big(\frac{\hbar}{k_{b_\theta}^2 - z_\theta^2} + \frac{1-\hbar}{k_{a_\theta}^2 - z_\theta^2}\Big)z_\theta(z_Q + y_Q) + \frac{3l_Q^{\frac{4}{3}}}{4}, \quad (44)$$

with $\tilde{\Xi}_Q = \Xi_Q - \underline{g}_Q\hat{\Xi}_Q$.

## IV. STABILITY ANALYSIS

*Theorem 1:* Consider the HFVs dynamics (1)-(7), control laws (16), (25), (30), (35), and (41), adaptation laws (15), (31), (36), and (40), and switching event-triggered mechanism (17) and (42). Given initial conditions satisfying that $L(0) \leq \Delta_1$, $z_\star(0) \in (-k_{a_\star}, k_{b_\star})$ where $\Delta_1 > \max\{k_{b_\star}, k_{a_\star}\}$ is a positive constant. Then, the following properties holds: 1) all closed-loop signals $z_\star$, $\tilde{\Xi}_V$, $\tilde{\Xi}_\gamma$, $\tilde{\Xi}_\theta$, $\tilde{\Xi}_Q$, $y_\gamma$, $y_\theta$, and $y_Q$ are semi-globally-uniformly-ultimately-bounded, and can converge to the residual sets within finite time $\overline{T} \leq \frac{1}{\kappa_1 p}\ln((2\kappa_1 L^p(0) + \kappa_2)/\kappa_2)$; 2) tracking errors $z_\star$ will always stay in the compact sets $\Omega_\star = \{z_\star : -k_{a_\star} \leq z_\star \leq k_{b_\star}\}$; 3) Zeno behavior is excluded.

*Proof:* See Appendix. ■

*Remark 4:* In the absence of fractional term on the Lyapunov expression of Lemma 1, finite-time stability is lost: in such a case it is still possible to let the trajectories converge into arbitrarily small regions, but no time guarantees can be given. Notice that if we choose $l = 1$ and $\tau_\star = 0$, the proposed finite-time control laws reduces to the standard (call it infinite-time) control laws:

$$\check{\Phi} = -(c_V + \kappa_V)z_V - \frac{\psi_V z_V^3\hat{\Xi}_V\Theta_V}{4l_V^4} - \frac{\psi_V\mu_V z_V^3}{4},$$
$$\gamma_d = -V^{-1}(c_h + \kappa_h)z_h - V^{-1}\dot{h}_{ref},$$
$$\theta_d = -(c_\gamma + \kappa_\gamma)z_\gamma - \frac{\psi_\gamma z_\gamma^3\hat{\Xi}_\gamma\Theta_\gamma}{4l_\gamma^4} - \frac{\psi_\gamma\mu_\gamma z_\gamma^3}{4},$$

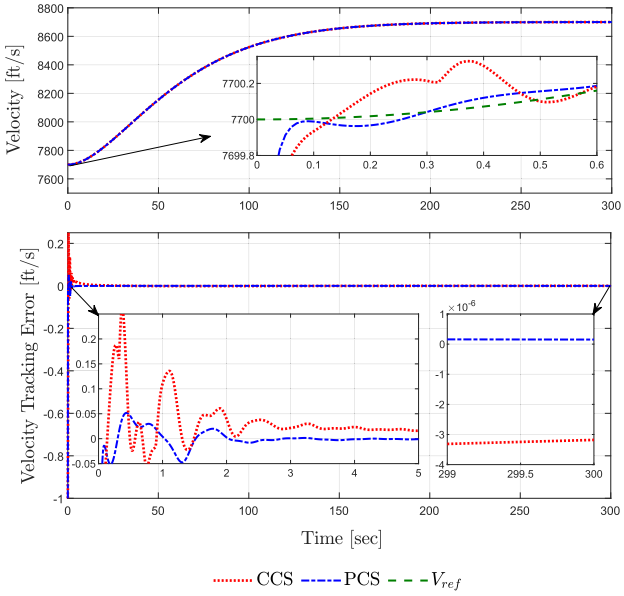


**FIGURE 3.** Tracking performances of velocity.

$$Q_d = -(c_\theta + \kappa_\theta)z_\theta - \frac{\psi_\theta z_\theta^3\hat{\Xi}_\theta\Theta_\theta}{4l_\theta^4} - \frac{\psi_\theta\mu_\theta z_\theta^3}{4},$$
$$\check{\delta}_e = -(c_Q + \kappa_Q)z_Q - \frac{\psi_Q z_Q^3\hat{\Xi}_Q\Theta_Q}{4l_Q^4} - \frac{\psi_Q\mu_Q z_Q^3}{4},$$

which are in line with the design in [20], [24]. For all these design, the convergence time cannot be prescribed.

## V. SIMULATION RESULTS

In this section, the proposed novel switching event-triggered finite-time control scheme (PFC) is compared with the conventional switching event-triggered infinite-time control scheme (CCS) [16] to validate its superiority in commend tracking performance. The vehicle climbs a maneuver from initial values $h = 88,000$ ft and $V = 7700$ ft/s to final values $h = 91,000$ ft and $V = 8700$ ft/s, respectively. The reference commands of $V_{ref}$ and $h_{ref}$ are generated using the following second-order filters with bandwidth 0.03rad/s and damping 0.95:

$$\frac{V_{ref}(s)}{V_c(s)} = \frac{h_{ref}(s)}{h_c(s)} = \frac{0.03^2}{s^2 + 2\times0.95\times0.03\times s + 0.03^2}. \quad (45)$$

The HFVs model parameter values are borrowed from [17], and the BLF parameters are set as $k_{a_V} = 2$, $k_{b_V} = 1$, $k_{a_h} = 5$, $k_{b_h} = 1$, $k_{a_\gamma} = 0.05$, $k_{b_\gamma} = 0.1$, $k_{a_\theta} = 0.1$, $k_{b_\theta} = 0.2$, $k_{a_Q} = 0.25$, and $k_{b_Q} = 0.5$. The control parameters are chosen as $c_V = 1.5$, $\mu_V = 2$, $\kappa_V = 1$, $c_h = 5$, $\mu_h = 2$, $\kappa_h = 0.5$, $c_\gamma = 2$, $\mu_\gamma = 1$, $\kappa_\gamma = 5$, $c_\theta = 1$, $\mu_\theta = 0.5$, $\kappa_\theta = 2$, $c_Q = 75$, $\mu_Q = 2$, $\kappa_Q = 3$, $l = 0.6$, $l_V = 1$, $l_\gamma = l_\theta = l_Q = 0.5$, $\tau_V = \tau_h = 0.01$, and $\tau_\gamma = \tau_\theta = \tau_Q = 0.001$. Parameters for event-triggered mechanism are given as $\rho_V = 0.015$, $\xi_V = 0.5$, $\kappa_{V,1} = 0.001$, $c_{V,0} = 0.0001$, $c_{V,1} = 0.007$,

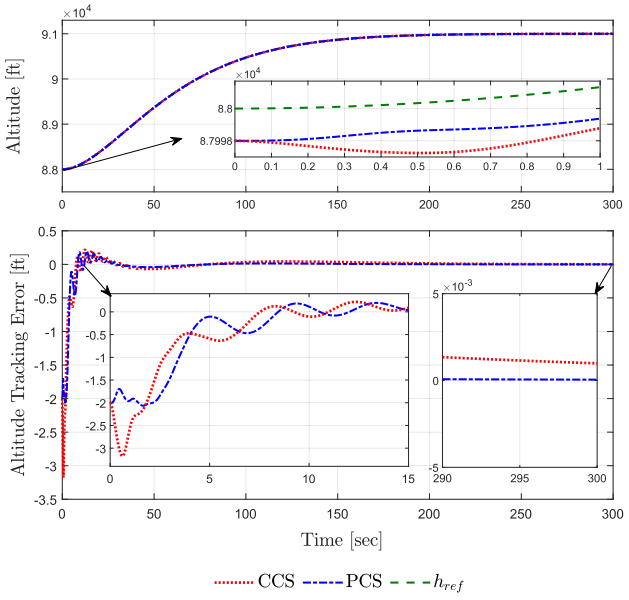


**FIGURE 4.** Tracking performances of altitude.

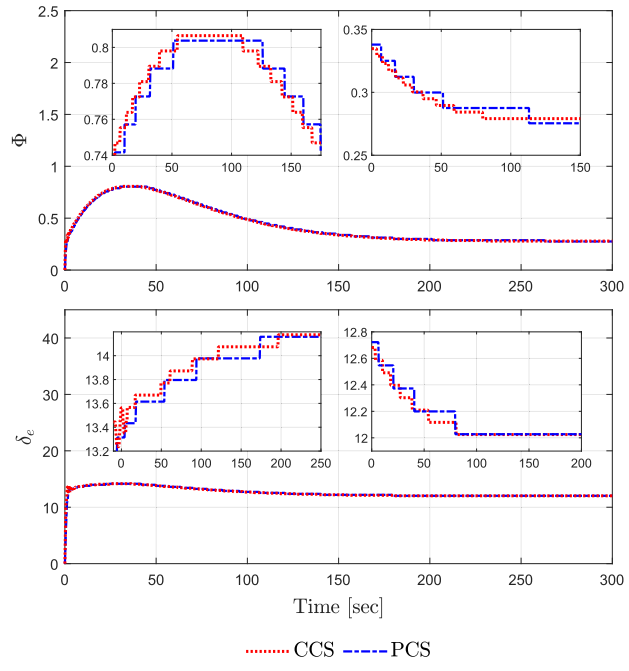


**FIGURE 5.** Event-triggered control inputs.

$\rho_h = 0.006$, $\xi_h = 13.5$, $\kappa_{h,1} = 0.02$, $c_{h,0} = 0.0001$, $c_{h,1} = 0.007$. Parameters for adaptive laws are chosen as $\rho_V = 0.5$, $\rho_\gamma = \rho_\theta = \rho_Q = 0.75$, $\sigma_{V1} = \sigma_{V2} = 0.75$, $\sigma_{\gamma 1} = \sigma_{\gamma 2} = \sigma_{\theta 1} = \sigma_{\theta 2} = 0.5$, and $\sigma_{Q1} = \sigma_{Q2} = 0.95$. The positive filter parameters are selected as $\tau_{\gamma 1} = \tau_{\theta 1} = \tau_{Q1} = 5$ and $\tau_{\gamma 2} = \tau_{\theta 2} = \tau_{Q2} = 2.5$. The initial system states are set as $V = 7699$ ft/s, $h = 87998$ ft, $\gamma = 0$ deg, $\theta = 1.6325$ deg, and $Q = 0$ deg/s, and the initial values of $\hat{\Xi}_V$, $\hat{\Xi}_\gamma$, $\hat{\Xi}_\theta$, and $\hat{\Xi}_Q$ are selected as zero.

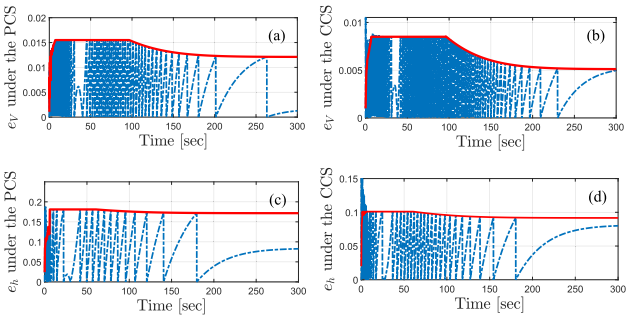


**FIGURE 6.** Sampling errors and triggering thresholds.

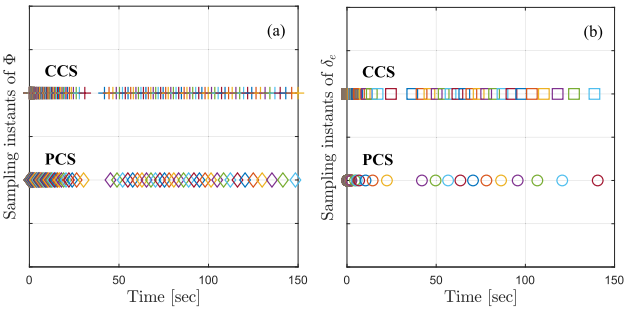


**FIGURE 7.** Sampling instants under two schemes.

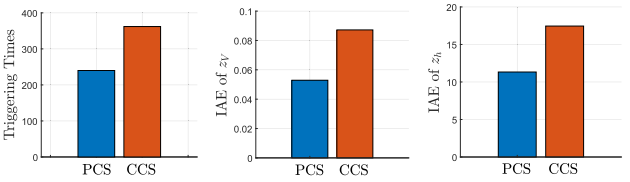


**FIGURE 8.** Triggering times under two schemes.

**TABLE 1.** Triggering times and performance indice.

| Control Schemes | Triggering Times | Performance indice IAE | |
|---|---|---|---|
| | | $e_V$ | $e_h$ |
| PCS | 240 | 0.0529 | 11.3282 |
| CCS | 362 | 0.0872 | 17.4531 |

The fuzzy rules in $\boldsymbol{W}_V^{*\mathrm{T}}\boldsymbol{\varphi}_V(\boldsymbol{x}_V)$ are listed as

$\mathcal{R}^l$: If $V$ is $F_V^i$, then $y$ is $B^l$, where $i = 1, 2, 3$; $l = 1, 2, 3$.

The fuzzy rules in $\boldsymbol{W}_\gamma^{*\mathrm{T}}\boldsymbol{\varphi}_\gamma(\boldsymbol{x}_\gamma)$ are listed as

$\mathcal{R}^l$: If $h$ is $F_h^i$, and $\gamma$ is $F_\gamma^j$, then $y$ is $B^l$, where $i = 1, 2, 3$; $j = 1, 2, 3$; $l = 1, 2, \ldots, 9$.

Then, the fuzzy rules in $\boldsymbol{W}_\theta^{*\mathrm{T}}\boldsymbol{\varphi}_\theta(\boldsymbol{x}_\theta)$ are listed as

$\mathcal{R}^l$: If $h$ is $F_h^i$, and $\gamma$ is $F_\gamma^j$, and $\theta$ is $F_\theta^k$, then $y$ is $B^l$, where $i = 1, 2, 3$; $j = 1, 2, 3$; $k = 1, 2, 3$; $l = 1, 2, \ldots, 27$.

The fuzzy rules in $\boldsymbol{W}_Q^{*\mathrm{T}}\boldsymbol{\varphi}_Q(\boldsymbol{x}_Q)$ are listed as

$\mathcal{R}^l$: If $h$ is $F_h^i$, and $\gamma$ is $F_\gamma^j$, and $\theta$ is $F_\theta^k$, and $Q$ is $F_Q^p$, then $y$ is $B^l$, where $i = 1, 2, 3$; $j = 1, 2, 3$; $k = 1, 2, 3$; $p = 1, 2, 3$; $l = 1, 2, \ldots, 81$.

The fuzzy membership function is given as follows:

$$\mu_{F_V^1}=\exp\left[-\frac{(V-7000)^2}{500}\right],\ \mu_{F_h^1}=\exp\left[-\frac{(h-80000)^2}{5000}\right],$$
$$\mu_{F_V^2}=\exp\left[-\frac{(V-8000)^2}{500}\right],\ \mu_{F_h^2}=\exp\left[-\frac{(h-85000)^2}{5000}\right],$$
$$\mu_{F_V^3}=\exp\left[-\frac{(V-9000)^2}{500}\right],\ \mu_{F_h^3}=\exp\left[-\frac{(h-90000)^2}{5000}\right],$$
$$\mu_{F_Q^1}=\exp\left[-\frac{(Q+0.03)^2}{0.002}\right],\ \mu_{F_\theta^1}=\exp\left[-\frac{(\theta-0)^2}{0.002}\right],$$
$$\mu_{F_Q^2}=\exp\left[-\frac{(Q-0)^2}{0.002}\right],\ \mu_{F_\theta^2}=\exp\left[-\frac{(\theta-0.02)^2}{0.002}\right],$$
$$\mu_{F_Q^3}=\exp\left[-\frac{(Q-0.03)^2}{0.002}\right],\ \mu_{F_\theta^3}=\exp\left[-\frac{(\theta-0.04)^2}{0.002}\right],$$
$$\mu_{F_\gamma^1}=\exp\left[-\frac{(\gamma-0)^2}{0.0005}\right],\ \mu_{F_\gamma^2}=\exp\left[-\frac{(\gamma-0.005)^2}{0.0005}\right],$$
$$\mu_{F_\gamma^3}=\exp\left[-\frac{(\gamma-0.01)^2}{0.0005}\right].$$

Simulation results can be seen in Figs. 3-8. The superiority of the proposed controller over CCS in both transient and steady-state performance is depicted in Figs. 3-4. The zooms in Fig. 5 shows the boundedness of event-triggered control inputs. Fig. 6 displays the trajectories of the sampling errors and the proposed triggering thresholds, which illustrates that the exponential term $\zeta_V(t)$ and $\zeta_h(t)$ give the larger triggering thresholds when tracking errors $z_V(t)$ and $z_h(t)$ become sufficiently small. Fig. 7 lists the sampling instants under two schemes, from which it can be seen that $t_{k+1}-t_k>0$, i.e., the proposed event-triggered mechanism is free from Zeno behavior. The total triggering times comparisons of two schemes are summarized in Fig. 8 and Table 1. It is apparent that the inter-execution time of the proposed triggering mechanism is longer than that of the conventional triggering mechanism [16]. Furthermore, integral absolute error (IAE) $\left[\int_0^T |e(t)|\mathrm{d}t\right]$ is utilized here as performance indice to evaluate the tracking performances of PCS and CCS quantitatively. The calculation results are summarized in Table 1, which showing that the performance indexe of PCS is smaller than that of CCS, i.e., our proposed control scheme can achieve more accurate tracking.

## VI. CONCLUSION

In this paper, an event-triggered fuzzy adaptive finite-time tracking control design is constructed for HFVs in the presence of asymmetric full state constraints. To alleviate the unnecessary communication resources waste, we skillfully devise a new switching event-triggered mechanism by embedding an exponential term into the event-triggered function. It is shown that the proposed event-triggered mechanism significantly reduces the frequencies of data transmission, especially when tracking errors become sufficiently small. In addition, a piecewise switching controller is constructed to avoid singularity issue typical of traditional recursive finite-time design methods.

## APPENDIX

Proof of Theorem 1: construct the entire Lyapunov function as follows

$$L=L_z+L_\Xi+L_y, \tag{46}$$

where

$$\begin{aligned}L_z=&\ L_V+L_h+L_\gamma+L_\theta+L_Q,\\ L_\Xi=&\ \frac{\tilde{\Xi}_V^2}{2\rho_V\underline{g}_V}+\frac{\tilde{\Xi}_\gamma^2}{2\rho_\gamma\underline{g}_\gamma}+\frac{\tilde{\Xi}_\theta^2}{2\rho_\theta}+\frac{\tilde{\Xi}_Q^2}{2\rho_Q\underline{g}_Q},\\ L_y=&\ \frac{1}{2}Vy_\gamma^2+\frac{\bar{g}_\gamma^2}{2\underline{g}_\gamma}y_\theta^2+\frac{1}{2}y_Q^2.\end{aligned}$$

Differentiating $L_y$ with respect to time, we arrive at

$$\begin{aligned}\dot{L}_y\le&\ y_Q\iota_Q\left(z_h,z_\gamma,z_\theta,z_Q,\hat{\Xi}_\gamma,y_\gamma,y_\theta,y_Q,h_{ref},\dot{h}_{ref},\ddot{h}_{ref}\right)\\&+\frac{\bar{g}_\gamma^2y_\theta}{\underline{g}_\gamma}\iota_\theta\left(z_h,z_\gamma,z_\theta,\hat{\Xi}_\gamma,y_\gamma,y_\theta,h_{ref},\dot{h}_{ref},\ddot{h}_{ref}\right)\\&+Vy_\gamma\iota_\gamma\left(z_h,z_\gamma,y_\gamma,\dot{h}_{ref},\ddot{h}_{ref}\right)-\tau_{\gamma2}Vy_\gamma^{l+1}\\&-\frac{\bar{g}_\gamma^2\tau_{\theta2}y_\theta^{l+1}}{\underline{g}_\gamma}-\frac{\bar{g}_\gamma^2\tau_{\theta1}y_\theta^2}{\underline{g}_\gamma}-\tau_{Q2}y_Q^{l+1}\\&-\tau_{Q1}y_Q^2-\tau_{\gamma1}Vy_\gamma^2.\end{aligned}\tag{47}$$

Construct a compact set as $\Omega_n=\{(z_V,z_h,z_\gamma,z_\theta,z_Q,\tilde{\Xi}_V,\tilde{\Xi}_\gamma,\tilde{\Xi}_\theta,\tilde{\Xi}_Q,y_\gamma,y_\theta,y_Q)|L(t)\le\Delta_1\}$, with $\Delta_1$ a positive constant. If $L(t)\le\Delta_1$, together with (47), we can deduce that $\iota_\star(\cdot)\le\Lambda_\star$ on the compact set $\Omega_n\times\Omega_{ref}$, where $\Lambda_\star$ is a positive constant, $\star$ denotes $\gamma$, $\theta$, and $Q$.

Then, invoking Young's inequality yields

$$\begin{aligned}\dot{L}\le&-\frac{\hbar c_V\underline{g}_Vz_V^2}{k_{b_V}^2-z_V^2}-\frac{(1-\hbar)c_V\underline{g}_Vz_V^2}{k_{a_V}^2-z_V^2}-\frac{(1-\hbar)\kappa_V\underline{g}_Vz_V\phi_V(z_V)}{k_{a_V}^2-z_V^2}\\&-\frac{\hbar\kappa_V\underline{g}_Vz_V\phi_V(z_V)}{k_{b_V}^2-z_V^2}-\frac{\sigma_{V1}\tilde{\Xi}_V^2}{2}-\sigma_{V2}\xi\,\tilde{\Xi}_V^{1+l}-\frac{\hbar c_hz_h^2}{k_{b_h}^2-z_h^2}\\&-\frac{\hbar\kappa_hz_h\phi_h(z_h)}{k_{b_h}^2-z_h^2}-\frac{(1-\hbar)c_hz_h^2}{k_{a_h}^2-z_h^2}-\frac{(1-\hbar)\kappa_hz_h\phi_h(z_h)}{k_{a_h}^2-z_h^2}\\&-\frac{(1-\hbar)\kappa_\gamma\underline{g}_\gamma z_\gamma\phi_\gamma(z_\gamma)}{k_{a_\gamma}^2-z_\gamma^2}-\frac{(1-\hbar)c_\gamma\underline{g}_\gamma z_\gamma^2}{k_{a_\gamma}^2-z_\gamma^2}-\frac{\hbar c_\gamma\underline{g}_\gamma z_\gamma^2}{k_{b_\gamma}^2-z_\gamma^2}\\&-\frac{\hbar\kappa_\gamma\underline{g}_\gamma z_\gamma\phi_\gamma(z_\gamma)}{k_{b_\gamma}^2-z_\gamma^2}-\sigma_{\gamma2}\xi\,\tilde{\Xi}_\gamma^{1+l}-\frac{\sigma_{\gamma1}\tilde{\Xi}_\gamma^2}{2}-\frac{\hbar c_\theta z_\theta^2}{k_{b_\theta}^2-z_\theta^2}\\&-\frac{(1-\hbar)\kappa_\theta z_\theta\phi_\theta(z_\theta)}{k_{a_\theta}^2-z_\theta^2}-\frac{(1-\hbar)c_\theta z_\theta^2}{k_{a_\theta}^2-z_\theta^2}-\frac{\hbar\kappa_\theta z_\theta\phi_\theta(z_\theta)}{k_{b_\theta}^2-z_\theta^2}\\&-\frac{\sigma_{\theta1}\tilde{\Xi}_\theta^2}{2}-\sigma_{\theta2}\xi\,\tilde{\Xi}_\theta^{1+l}-\frac{(1-\hbar)c_Q\underline{g}_Qz_Q^2}{k_{a_Q}^2-z_Q^2}-\frac{\hbar c_Q\underline{g}_Qz_Q^2}{k_{b_Q}^2-z_Q^2}\end{aligned}$$

$$-\frac{\hbar\kappa_Q \underline{g}_Q z_Q \phi_Q(z_Q)}{k_{b_Q}^2 - z_Q^2} - \frac{(1-\hbar)\kappa_Q \underline{g}_Q z_Q \phi_Q(z_Q)}{k_{a_Q}^2 - z_Q^2} + d$$
$$-\frac{\sigma_{Q1}\tilde{\Xi}_Q^2}{2} - \sigma_{Q2}\xi\,\tilde{\Xi}_Q^{1+l} - \tau_{\gamma 2} y_\gamma^{l+1} - \tau_{\theta 2} y_\theta^{l+1}$$
$$-\tau_{Q2} y_Q^{l+1} - \widehat{\tau}_{\gamma 1} y_\gamma^2 - \widehat{\tau}_{\theta 1} y_\theta^2 - \widehat{\tau}_{Q1} y_Q^2, \tag{48}$$

where $\widehat{\tau}_{Q1} = \tau_{Q1} - 1/(2\chi_Q)$, $\widehat{\tau}_{\theta 1} = \bar{g}_\gamma^2/\underline{g}_\gamma\big(\tau_{\theta 1} - 1/(2\chi_\theta)\big)$, $\widehat{\tau}_{\gamma 1} = V\big(\tau_{\gamma 1} - 1/(2\chi_\gamma)\big)$, $d = (\sigma_{V1}\Xi_V^2 + \sigma_{\gamma 1}\Xi_\gamma^2 + \sigma_{\theta 1}\Xi_\theta^2 + \sigma_{Q1}\Xi_Q^2)/2 + (3l_V^{\frac{4}{3}} + 3l_\gamma^{\frac{4}{3}} + 3l_\theta^{\frac{4}{3}} + 3l_Q^{\frac{4}{3}})/4 + 3\varepsilon_V^{*\frac{4}{3}}/\big(4(\mu_V \underline{g}_V)^{\frac{1}{3}}\big) + 3\varepsilon_\gamma^{*\frac{4}{3}}/(4(\mu_\gamma \underline{g}_\gamma)^{\frac{1}{3}}) + 3\varepsilon_\theta^{*\frac{4}{3}}/(4(\mu_\theta \underline{g}_\theta)^{\frac{1}{3}}) + 3\varepsilon_Q^{*\frac{4}{3}}/(4(\mu_Q \underline{g}_Q)^{\frac{1}{3}}) + \sigma_{V2}\zeta\,\Xi_V^{1+l} + \sigma_{\gamma 2}\zeta\,\Xi_\gamma^{1+l} + \sigma_{\theta 2}\zeta\,\Xi_\theta^{1+l} + \sigma_{Q2}\zeta\,\Xi_Q^{1+l} + V\chi_\gamma\Lambda_\gamma^2/2 + \bar{g}_\gamma^2\chi_\theta\Lambda_\theta^2/(2\underline{g}_\gamma) + \chi_Q\Lambda_Q^2/2$ with $\chi_\gamma$, $\chi_\theta$, $\chi_Q$ being positive constants, and $\xi$, $\zeta$ being defined in Lemma 2. Here we choose $\tau_{\gamma 1} > 1/(2\chi_\gamma)$, $\tau_{\theta 1} > 1/(2\chi_\theta)$, and $\tau_{Q1} > 1/(2\chi_Q)$ such that $\widehat{\tau}_{\gamma 1} > 0$, $\widehat{\tau}_{\theta 1} > 0$, and $\widehat{\tau}_{Q1} > 0$.

From the definition of $\phi_\star(z_\star)$, let us consider the following two cases:

Case 1: When $|z_\star| < \tau_\star$, differentiating $L$ yields

$$\dot{L} \le -\frac{\hbar c_V \underline{g}_V z_V^2}{k_{b_V}^2 - z_V^2} - \frac{(1-\hbar)c_V \underline{g}_V z_V^2}{k_{a_V}^2 - z_V^2} - \frac{\hbar c_h z_h^2}{k_{b_h}^2 - z_h^2} + d$$
$$-\frac{(1-\hbar)c_h z_h^2}{k_{a_h}^2 - z_h^2} - \frac{\hbar c_\gamma \underline{g}_\gamma z_\gamma^2}{k_{b_\gamma}^2 - z_\gamma^2} - \frac{(1-\hbar)c_\gamma \underline{g}_\gamma z_\gamma^2}{k_{a_\gamma}^2 - z_\gamma^2}$$
$$-\frac{\hbar c_\theta z_\theta^2}{k_{b_\theta}^2 - z_\theta^2} - \frac{(1-\hbar)c_\theta z_\theta^2}{k_{a_\theta}^2 - z_\theta^2} - \frac{(1-\hbar)c_Q \underline{g}_Q z_Q^2}{k_{a_Q}^2 - z_Q^2}$$
$$-\frac{\sigma_{V1}\tilde{\Xi}_V^2}{2} - \frac{\sigma_{\gamma 1}\tilde{\Xi}_\gamma^2}{2} - \frac{\sigma_{\theta 1}\tilde{\Xi}_\theta^2}{2} - \frac{\sigma_{Q1}\tilde{\Xi}_Q^2}{2}$$
$$-\frac{\hbar c_Q \underline{g}_Q z_Q^2}{k_{b_Q}^2 - z_Q^2} - \widehat{\tau}_{\gamma 1} y_\gamma^2 - \widehat{\tau}_{\theta 1} y_\theta^2 - \widehat{\tau}_{Q1} y_Q^2. \tag{49}$$

The above inequality can be rewritten as

$$L \le L(0)\exp\left(-\frac{\varpi}{\omega}t\right) + \frac{d\omega}{\varpi}. \tag{50}$$

where $\varpi = \min\big\{c_V \underline{g}_V, c_h, c_\gamma \underline{g}_\gamma, c_\theta, c_Q \underline{g}_Q, \sigma_{V1}/2, \sigma_{\gamma 1}/2, \sigma_{\theta 1}/2, \sigma_{Q1}/2, \widehat{\tau}_{\gamma 1}, \widehat{\tau}_{\theta 1}, \widehat{\tau}_{Q1}\big\}$, and $\omega = \min\big\{1/(2\rho_V \underline{g}_V), 1/2, 1/(2\rho_\gamma \underline{g}_\gamma), V/2, 1/(2\rho_\theta), 1/(2\rho_Q \underline{g}_Q), \bar{g}_\gamma^2/2\underline{g}_\gamma\big\}$.

Case 2: When $|z_\star| \ge \tau_\star$, differentiating $L$ yields

$$\dot{L} \le -\frac{\hbar c_V \underline{g}_V z_V^2}{k_{b_V}^2 - z_V^2} - \frac{(1-\hbar)c_V \underline{g}_V z_V^2}{k_{a_V}^2 - z_V^2} - \hbar\kappa_V \underline{g}_V \left(\frac{z_V^2}{k_{b_V}^2 - z_V^2}\right)^q$$
$$-(1-\hbar)\kappa_V \underline{g}_V \left(\frac{z_V^2}{k_{a_V}^2 - z_V^2}\right)^q - \frac{\sigma_{V1}\tilde{\Xi}_V^2}{2} - \sigma_{V2}\xi\,\tilde{\Xi}_V^{1+l}$$
$$-\frac{\hbar c_h z_h^2}{k_{b_h}^2 - z_h^2} - \hbar\kappa_h \left(\frac{z_h^2}{k_{b_h}^2 - z_h^2}\right)^q - (1-\hbar)\kappa_h \left(\frac{z_h^2}{k_{b_h}^2 - z_h^2}\right)^q$$
$$-\frac{(1-\hbar)c_h z_h^2}{k_{a_h}^2 - z_h^2} - (1-\hbar)\kappa_\gamma \underline{g}_\gamma \left(\frac{z_\gamma^2}{k_{b_\gamma}^2 - z_\gamma^2}\right)^q - \frac{\hbar c_\gamma \underline{g}_\gamma z_\gamma^2}{k_{b_\gamma}^2 - z_\gamma^2}$$
$$-\frac{(1-\hbar)c_\gamma \underline{g}_\gamma z_\gamma^2}{k_{a_\gamma}^2 - z_\gamma^2} - \hbar\kappa_\gamma \underline{g}_\gamma \left(\frac{z_\gamma^2}{k_{b_\gamma}^2 - z_\gamma^2}\right)^q - \sigma_{\gamma 2}\xi\,\tilde{\Xi}_\gamma^{1+l}$$
$$-\frac{\sigma_{\gamma 1}\tilde{\Xi}_\gamma^2}{2} - \frac{\hbar c_\theta z_\theta^2}{k_{b_\theta}^2 - z_\theta^2} - \frac{(1-\hbar)c_\theta z_\theta^2}{k_{a_\theta}^2 - z_\theta^2} - \hbar\kappa_\theta \left(\frac{z_\theta^2}{k_{b_\theta}^2 - z_\theta^2}\right)^q$$
$$-(1-\hbar)\kappa_\theta \left(\frac{z_\theta^2}{k_{b_\theta}^2 - z_\theta^2}\right)^q - \frac{\sigma_{\theta 1}\tilde{\Xi}_\theta^2}{2} - \frac{(1-\hbar)c_Q \underline{g}_Q z_Q^2}{k_{a_Q}^2 - z_Q^2}$$
$$-\sigma_{\theta 2}\xi\,\tilde{\Xi}_\theta^{1+l} - \frac{\hbar c_Q \underline{g}_Q z_Q^2}{k_{b_Q}^2 - z_Q^2} - \hbar\kappa_Q \underline{g}_Q \left(\frac{z_Q^2}{k_{b_Q}^2 - z_Q^2}\right)^q + d$$
$$-(1-\hbar)\kappa_Q \underline{g}_Q \left(\frac{z_Q^2}{k_{b_Q}^2 - z_Q^2}\right)^q - \frac{\sigma_{Q1}\tilde{\Xi}_Q^2}{2} - \sigma_{Q2}\xi\,\tilde{\Xi}_Q^{1+l}$$
$$-\tau_{\gamma 2} y_\gamma^{l+1} - \tau_{\theta 2} y_\theta^{l+1} - \tau_{Q2} y_Q^{l+1}$$
$$-\widehat{\tau}_{\gamma 1} y_\gamma^2 - \widehat{\tau}_{\theta 1} y_\theta^2 - \widehat{\tau}_{Q1} y_Q^2, \tag{51}$$

Defining $\chi = \min\big\{c_V \underline{g}_V, c_\gamma \underline{g}_\gamma, c_Q \underline{g}_Q, c_h, c_\theta, \widehat{\tau}_{\gamma 1}, \widehat{\tau}_{\theta 1}, \widehat{\tau}_{Q1}, \sigma_{V1}/2, \sigma_{\gamma 1}/2, \sigma_{\theta 1}/2, \sigma_{Q1}/2\big\}$, $\lambda = \min\big\{\kappa_V \underline{g}_V, \kappa_h, \kappa_\theta, \kappa_\gamma \underline{g}_\gamma, \kappa_Q \underline{g}_Q, \sigma_{V2}\xi, \sigma_{\gamma 2}\xi, \sigma_{\theta 2}\xi, \sigma_{Q2}\xi, \tau_{\gamma 2}, \tau_{\theta 2}, \tau_{Q2}\big\}$, and following from (46) and (51) that

$$\dot{L} \le -\kappa_1 L - \kappa_2 L^q + d, \tag{52}$$

where $\kappa_1 = \chi/\omega$ and $\kappa_2 = \lambda/\omega^q$.

According to Theorem 5.2 of [25], there exists a finite time $\bar{t}$ satisfying $L \ge (2d/\kappa_2)^{(1/q)}$ for all $t \in [0, \bar{t}]$. As a result, for all $t \in [0, \bar{t}]$, we have $\dot{L} \le -\kappa_1 L - \kappa_2 L^q/2$. Invoking to Lemma 1 we can get the fast finite-time stability of the closed-loop system within a finite time $\overline{T} \le \frac{1}{\kappa_1 p}\ln\big((2\kappa_1 L^p(0) + \kappa_2)/\kappa_2\big)$. In addition, we can deduce that $\bar{t} \le \overline{T}$. Thus, for $\forall t > \overline{T}$, $L \le (2d/\kappa_2)^{(1/q)}$. As such, all error signals will converge into the following compact sets:

$$\begin{cases} z_\star \le k_{b_\star}\sqrt{1 - \exp\left(-2\,(2d/\kappa_2)^{\frac{1}{q}}\right)}, \\ z_\star \ge -k_{a_\star}\sqrt{1 - \exp\left(-2\,(2d/\kappa_2)^{\frac{1}{q}}\right)}, \\ |\tilde{\Xi}_V| \le \sqrt{2\rho_V \underline{g}_V}\,(2d/\kappa_2)^{\frac{1}{q}}, \quad |\tilde{\Xi}_\gamma| \le \sqrt{2\rho_\gamma \underline{g}_\gamma}\,(2d/\kappa_2)^{\frac{1}{q}}, \\ |\tilde{\Xi}_Q| \le \sqrt{2\rho_Q \underline{g}_Q}\,(2d/\kappa_2)^{\frac{1}{q}}, \quad |\tilde{\Xi}_\theta| \le \sqrt{2\rho_\theta}\,(2d/\kappa_2)^{\frac{1}{q}}, \\ |y_\theta| \le \sqrt{2\underline{g}_\gamma/\bar{g}_\gamma^2}\left(2d/\kappa_2\right)^{\frac{1}{2q}}, \quad |y_\gamma| \le \sqrt{2/V}\,(2d/\kappa_2)^{\frac{1}{q}}, \\ |y_Q| \le \sqrt{2}\,(2d/\kappa_2)^{\frac{1}{q}}, \end{cases} \tag{53}$$

in finite time. To prove that the constraints are never violated. we can resort to Lemma 1 of [26], (50), and (53) to conclude that $z_\star \in (-k_{a_\star}, k_{b_\star})$ for $\forall t > 0$. In addition, according to switching event-triggered mechanism (17) and (42), the next event will not be triggered before $e_V(t_k, t) = \kappa_{V,1}$ and $e_h(t_k, t) = \kappa_{h,1}$. Thence, a minimum time interval between two adjacent events is existent, indicating that no Zeno behavior occurs. ■

## REFERENCES


[1] W. Wang, Z. Hou, S. Shan, and L. Chen, "Periodically cruising hypersonic vehicle with active cooling: An optimal-control based design approach," *IEEE Access*, vol. 7, pp. 65486–65505, 2019.

[2] X. Bu, "Air-breathing hypersonic vehicles funnel control using neural approximation of non-affine dynamics," *IEEE/ASME Trans. Mechatronics*, vol. 23, no. 5, pp. 2099–2108, Oct. 2018.

[3] Y. Xie, X. Zhuang, Z. Xi, and H. Chen, "Dual-channel and bidirectional neural network for hypersonic glide vehicle trajectory prediction," *IEEE Access*, vol. 9, pp. 92913–92924, 2021.

[4] R. Zuo, Y. Li, M. Lv, Z. Liu, and Z. Dong, "Design of singularity-free fixed-time fault-tolerant control for HFVs with guaranteed asymmetric time-varying flight state constraints," *Aerosp. Sci. Technol.*, vol. 120, Jan. 2022, Art. no. 107270.

[5] F. Guo and P. Lu, "Improved adaptive integral-sliding-mode fault-tolerant control for hypersonic vehicle with actuator fault," *IEEE Access*, vol. 9, pp. 46143–46151, 2021.

[6] S. Tan, J. Li, and H. Lei, "Robust control of air-breathing hypersonic vehicles with adaptive projection-based parameter estimation," *IEEE Access*, vol. 7, pp. 88998–89013, 2019.

[7] Q. Shen, B. Jiang, and V. Cocquempot, "Fault-tolerant control for T–S fuzzy systems with application to near-space hypersonic vehicle with actuator faults," *IEEE Trans. Fuzzy Syst.*, vol. 20, no. 4, pp. 652–665, Aug. 2012.

[8] L. Fiorentini, A. Serrani, M. A. Bolender, and D. B. Doman, "Nonlinear robust adaptive control of flexible air-breathing hypersonic vehicles," *J. Guid., Control, Dyn.*, vol. 32, no. 2, pp. 401–416, Mar. 2009.

[9] K. Li, S. Tong, and Y. Li, "Finite-time adaptive fuzzy decentralized control for nonstrict-feedback nonlinear systems with output-constraint," *IEEE Trans. Syst., Man, Cybern. Syst.*, vol. 50, no. 12, pp. 5271–5284, Dec. 2020, doi: 10.1109/TSMC.2018.2870698.

[10] S. Sui, C. L. P. Chen, and S. Tong, "Fuzzy adaptive finite-time control design for nontriangular stochastic nonlinear systems," *IEEE Trans. Fuzzy Syst.*, vol. 27, no. 1, pp. 172–184, Jan. 2019.

[11] J. Xia, H. Gao, M. Liu, G. Zhuang, and B. Zhang, "Non-fragile finite-time extended dissipative control for a class of uncertain discrete time switched linear systems," *J. Franklin Inst.*, vol. 355, no. 6, pp. 3031–3049, Apr. 2018.

[12] J. H. Kim and S. J. Yoo, "Distributed event-triggered adaptive formation tracking of networked uncertain stratospheric airships using neural networks," *IEEE Access*, vol. 8, pp. 49977–49988, 2020.

[13] L. Xu, H. Ma, and S. Xiao, "Exponential synchronization of chaotic Lur'e systems using an adaptive event-triggered mechanism," *IEEE Access*, vol. 6, pp. 61295–61304, 2018.

[14] Q. Hu, Y. Shi, and C. Wang, "Event-based formation coordinated control for multiple spacecraft under communication constraints," *IEEE Trans. Syst., Man, Cybern., Syst.*, vol. 51, no. 5, pp. 3168–3179, May 2021, doi: 10.1109/TSMC.2019.2919027.

[15] W. Wang, C. Wen, J. Huang, and J. Zhou, "Adaptive consensus of uncertain nonlinear systems with event triggered communication and intermittent actuator faults," *Automatica*, vol. 111, Jan. 2020, Art. no. 108667.

[16] L. Xing, C. Wen, Z. Liu, H. Su, and J. Cai, "Event-triggered adaptive control for a class of uncertain nonlinear systems," *IEEE Trans. Autom. Control*, vol. 62, no. 4, pp. 2071–2076, Apr. 2017.

[17] J. T. Parker, A. Serrani, S. Yurkovich, M. A. Bolender, and D. B. Doman, "Control-oriented modeling of an air-breathing hypersonic vehicle," *J. Guid., Control, Dyn.*, vol. 30, no. 3, pp. 856–869, May 2007.

[18] R. Zuo, Y. Li, M. Lv, and Z. Liu, "Realization of trajectory precise tracking for hypersonic flight vehicles with prescribed performances," *Aerosp. Sci. Technol.*, vol. 111, Apr. 2021, Art. no. 106554.

[19] M. Lv, Y. Li, W. Pan, and S. Baldi, "Finite-time fuzzy adaptive constrained tracking control for hypersonic flight vehicles with singularity-free switching," *IEEE/ASME Trans. Mechatronics*, vol. 27, no. 3, pp. 1594–1605, Jun. 2022, doi: 10.1109/TMECH.2021.3090509.

[20] X. Bu, Y. Xiao, and H. Lei, "An adaptive critic design-based fuzzy neural controller for hypersonic vehicles: Predefined behavioral nonaffine control," *IEEE/ASME Trans. Mechatron.*, vol. 24, no. 4, pp. 1871–1881, Jul. 2019.

[21] S. Yu, X. Yu, B. Shirinzadeh, and Z. Man, "Continuous finite-time control for robotic manipulators with terminal sliding mode," *Automatica*, vol. 41, no. 11, pp. 1957–1964, Nov. 2005.

[22] Y. Wang, Y. Song, M. Krstic, and C. Wen, "Fault-tolerant finite time consensus for multiple uncertain nonlinear mechanical systems under single-way directed communication interactions and actuation failures," *Automatica*, vol. 63, pp. 374–383, Jan. 2016.

[23] R. Zuo, Y. Li, M. Lv, Z. Liu, and F. Zhang, "Fuzzy adaptive output-feedback constrained trajectory tracking control for HFVs with fixed-time convergence," *IEEE Trans. Fuzzy Syst.*, early access, Mar. 23, 2022, doi: 10.1109/TFUZZ.2022.3161732.

[24] K. P. Tee, S. S. Ge, and E. H. Tay, "Barrier Lyapunov functions for the control of output-constrained nonlinear systems," *Automatica*, vol. 45, no. 4, pp. 918–927, Apr. 2009.

[25] S. P. Bhat and D. S. Bernstein, "Finite-time stability of continuous autonomous systems," *SIAM J. Control Optim.*, vol. 38, no. 3, pp. 751–766, Jan. 2000.

[26] B. Ren, S. S. Ge, K. P. Tee, and T. H. Lee, "Adaptive neural control for output feedback nonlinear systems using a barrier Lyapunov function," *IEEE Trans. Neural Netw.*, vol. 21, no. 8, pp. 1339–1345, Aug. 2010.